DYNAMIC BEHAVIOR OF THE HTR-10 REACTOR: DUAL TEMPERATURE FEEDBACK MODEL

by

Seyed Ali HOSSEINI

Young Researchers and Elites Club, Abhar Branch, Islamic Azad University, Abhar, Iran

Scientific paper
DOI: 10.2298/NTRP1502124H

The current work aims at presenting a simple model for PBM-type reactors' dynamic behavior analysis. The proposed model is based on point kinetics equations coupled with feedbacks from fuel and moderator temperatures. The temperature reactivity coefficients were obtained through MCNP code and via available experimental data. Parameters such as heat capacity and heat conductivity were carefully analyzed and the final system of equations was numerically solved. The obtained results, while in partial agreement with previously proposed models, suggest lower sensitivity to step reactivity insertion as compared to other reactor designs and inherent safety of the design.

Key words: HTR-10, point kinetic model, temperature reactivity coefficient, MCNP, pebble-bed modular reactor

INTRODUCTION

Due to their innate safety, operation flexibility, energy, cost, and time efficiency, pebble-bed type high temperature gas-graphite reactors are one of the most promising 4th generation reactor core designs to date. Negative temperature coefficient factors – fuel, moderator, and total – along with the TRISO coating technology and a very flexible fuel management system, all guarantee the safe operation of these units during their lifetime. This design is known to yield high burn-up values – compared to typical PWR and BWR units. The high operating temperature of this reactor type gives the operator the possibility to use the remainder of the generated thermal energy in water processing units and thus achieve considerably higher effective energy efficiency [1-4].

The HTR-10 was one of the first PBM-type reactors to go critical and operate. This reactor unit is a 10 MW research reactor located in Tsinghua, China. Since its first criticality in 2003, many research groups modelled it using a variety of codes such as MCNP [5]. The current work intends to model the dynamic behavior of the HTR-10 in response to a step reactivity insertion. Given the fuel handling system, such an increase in reactivity will be equivalent to the insertion of new pebbles into the core.

Criticality analysis of the reactor core at different fuel and moderator temperatures and pebble-filled core heights in order to establish a relation between the reactor core multiplication factor and temperature would be the first step toward a model representing the dynamic behavior of the reactor. The obtained temperature reactivity coefficients will be used in establishing the system of equations of the HTR-10 relating parameters such as fuel and moderator temperature, neutron density and reactivity.

REACTOR CORE MODELLING AND TEMPERATURE REACTIVITY CALCULATION

A methodologically correct, reliable, and accurate modeling of such a system requires both a complete and benchmarked cross-section library covering a wide range of temperatures and a correct geometrical model of the reactor core. The default MCNP4c library only covers room temperature and is based on an older version of the ENDF-series cross-section library, ENDF V. Hence, in order to be able to perform multiplication factor calculations at different temperatures and obtain more accurate results, we took advantage of the ADS 2.0 library [6] based on ENDF-VII cross-sections [7]. The effect of this new cross-section library on PBM-type reactor criticality analysis with MCNP4c has previously been investigated [8].

Modelling the unusual structure of PBM-type reactors is one of the challenges in criticality calculations [9]. The double heterogeneous nature of the reactor core – consisting of fuel particles inside fuel pebbles and pebbles inside the reactor core – is usually the

* Corresponding author; e-mail: hosseiniabhari@gmail.com

source of difficulties in geometrical modelling. The first level of difficulties has to do with the distribution of fuel particles inside the fuel pebbles. The particles could be modelled and individually placed so as to achieve random distribution or by using an appropriate unit cell lattice. Given the large number of fuel particles per fuel pebble, approximately 8335, MCNP code limitations on the total number of surfaces and cells and the limited effect of fuel particle distribution on the multiplication factor, an array of simple cubic unit cells seems to be the best choice [10]. Fuel and dummy pebbles' distribution inside the core, on the other hand, has been shown to strongly affect the multiplication factor. The large discrepancies in multiplication factors obtained using different pebble placement schemes are an undeniable proof of the previous statement. These rather large variations, attesting to the undeniable effect of pebble distribution on the multiplication factor, also put emphasis on the stochastic nature of the multiplication factor for a PBM-type reactor. Therefore, to avoid any error in the process, one should run the problem for a number of distributions and report a mean value and a standard deviation. The variations arising from the pebble distribution inside the core have been shown to be largely superior to code-induced deviations [11].

A variety of innovative distribution methods have been proposed over the past years. This work made use of a model proposed by the author in previous works[11]. The model takes account of both the random mixture of fuel and dummy pebbles and the random distribution of void regions inside the core. A sample core produced using this model is displayed in figs. 1 and 2.

Temperature reactivity coefficients are usually obtained by calculating the reactor multiplication factor at different temperatures and taking the derivative

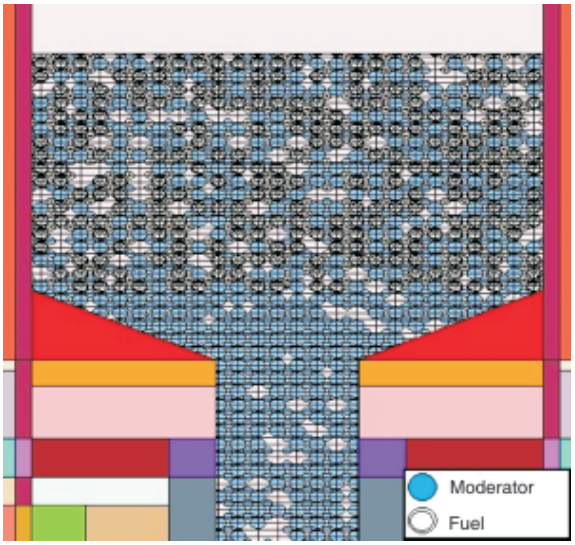

Figure 1. Vertical cross-section of the reactor core

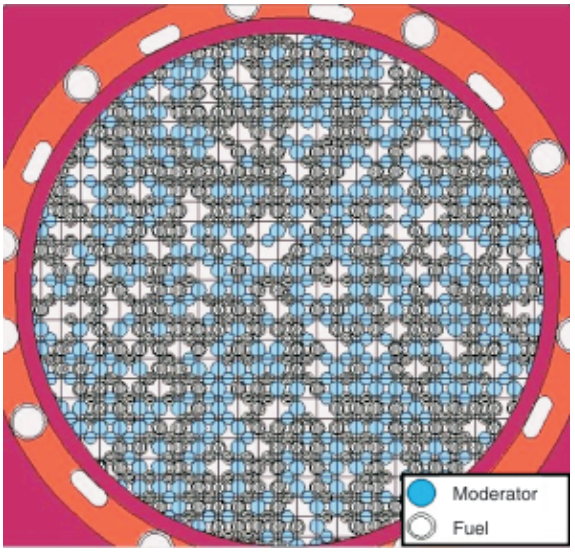

Figure 2. Horizontal cross-section of the reactor core's upper region

$$\alpha_T \quad \frac{\mathrm{d}\,\frac{1}{k}}{\mathrm{d}T} \quad \frac{1}{k}\frac{\mathrm{d}k}{\mathrm{d}T} \quad \frac{\mathrm{d}\rho}{\mathrm{d}T} \quad k \quad 1 \qquad (1)$$

The simulations were performed for different pebble-filled heights -different number of pebbles and different fuel and moderator temperatures. The results of these simulations are presented in figs. 3-6.

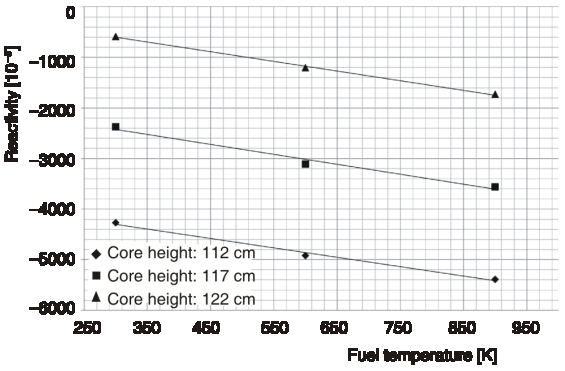

Figure 3. Reactivity variations as a function of fuel temperature

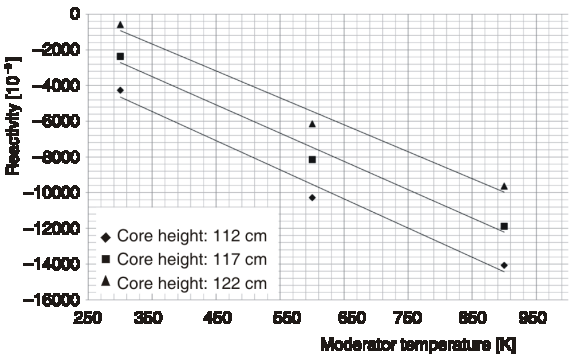

Figure 4. Reactivity variations as a function of moderator temperature

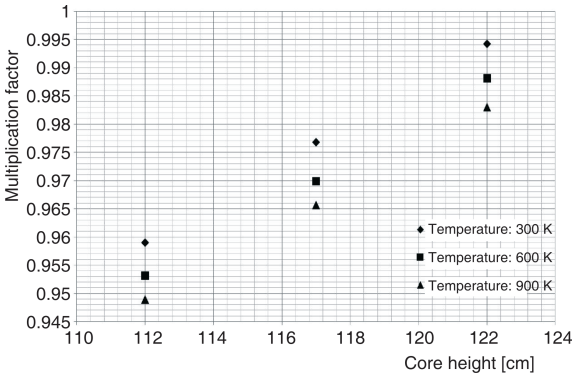

Figure 5. Variations of the multiplication factor with the reactor core's pebble-filled height at various fuel temperatures

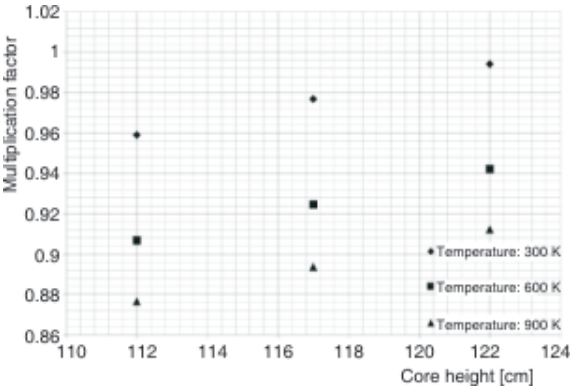

Figure 6. Variations of the multiplication factor with the reactor core's pebble-filled height at various moderator temperatures

As expected, the obtained results are in agreement with experimental data. The fuel temperature reactivity coefficient is approximately equal to $-1.9\ 10^{-5}\ K^{-1}$, while the moderator reactivity coefficient is $-15.7\ 10^{-5}\ K^{-1}$ [9, 12].

THE KINETIC MODEL

Point kinetic equations constitute the first part of the reactor's dynamic behavior model. The PKE model is usually represented through these two equations [13]

$$\frac{dn(t)}{dt} = \frac{\rho(t) - \beta}{\Lambda} n(t) + \sum_{i=1}^{6} \lambda_i C_i(t) + q(t) \quad (2)$$

$$\frac{dC_i(t)}{dT} = \frac{\beta_i}{\Lambda} n(t) - \lambda_i C_i(t) \quad i = 1,\ldots,6 \quad (3)$$

where we have made use of the following notation: $n(t)$ is the power, $\rho(t)$ – time dependent reactivity, $C_i(t)$ – the i-th group power [13, 14], β_i – the delayed neutron fraction in group i, Λ – the prompt neutron generation time, $q(t)$ – the neutron source term, and β – the total delayed neutron fraction.

There are no neutron sources inside the core and, to simplify the equations, the model will be a one--group delayed neutron model. Therefore,

$$\frac{dn(t)}{dt} = \frac{\rho(t) - \beta}{\Lambda} n(t) + \lambda C(t) \quad (4)$$

$$\frac{dC(t)}{dt} = \frac{\beta}{\Lambda} n(t) - \lambda C(t) \quad (5)$$

where we have [14]

$$\frac{1}{\lambda} = \frac{1}{\beta} \sum_{i=1}^{6} \frac{\beta_i}{\lambda_i} \quad (6)$$

Given the fact that the present work is concerned with the dynamic behavior of the HTR-10, in response to a step reactivity input one can define $\rho(t)$ as follows

$$\rho(t) = \rho_0 + \rho_{\text{temperature feedback}}(t) \quad (7)$$

Making use of the fuel and moderator temperature reactivity coefficients, we have

$$\rho(t) = \rho_0(t) + \alpha_F [T_F(t) - T_F(0)] + \alpha_M [T_M(t) - T_M(0)] \quad (8)$$

where α_F is the fuel temperature reactivity coefficient, α_M – the moderator temperature reactivity coefficient, T_F – the fuel temperature, and T_M – the moderator temperature.

Both the fuel and moderator temperature are time-varying parameters. In order to establish an equation relating these variables to the reactor's neutronic parameters and their behavior, one must perform an energy balance analysis in both regions. For the fuel region, the equation consists of an energy production term caused by ^{235}U fission and an energy loss term – energy lost to the moderator region through conduction, hence

$$m_F C_{pF} \frac{dT_F(t)}{dt} = n(t) - U[T_F(t) - T_M(t)] \quad (9)$$

$$U = N_F \frac{4\pi}{\frac{r_2 - r_1}{k_2 r_1 r_2} + \frac{r_3 - r_2}{k_3 r_2 r_3} + \frac{r_4 - r_3}{k_4 r_3 r_4} + \frac{r_5 - r_4}{k_5 r_4 r_5}} \quad (10)$$

where U is the total conductance between the fuel and moderator regions, r_1 through r_5 – the radius of each region between the fuel kernel and the moderator, k_2 – through k_5 – the thermal conductivity coefficient of the aforementioned regions, m_F – the fuel region mass, and C_{pF} – the fuel heat capacity.

The geometrical model of the fuel particle along with the different regions and their thermal properties are displayed in fig. 7 and tab. 1[12].

On the other hand, the moderator region gains energy from the fuel region through conduction and loses energy to the coolant through convection. Therefore

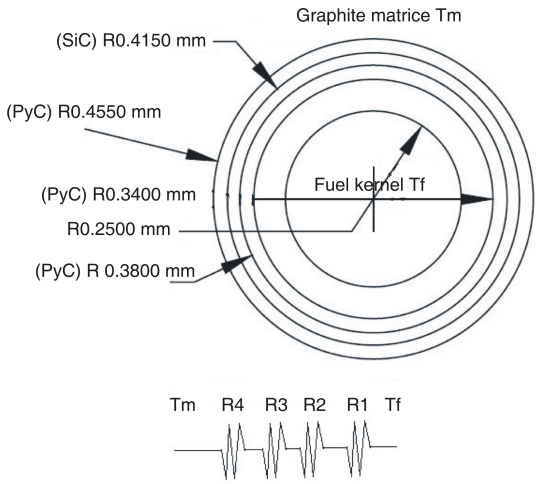

Figure 7. Fuel particle geometrical structure
PyC – pyrolitic carbon, SiC – silicon carbid

Table 1. TRISO layers properties

Region	Material	Thickness [mm]	Thermal conductivity [$Wm^{-1}K^{-1}$]
Coating 1	Porous pyrolytic carbon	0.09	0.5
Coating 2	Inner pyrolytic carbon	0.04	4.0
Coating 3	Silicon carbide	0.035	16.0
Coating 4	Outer pyrolytic carbon	0.04	4.0

$$m_{\mathrm{M}} C_{p\mathrm{M}} \frac{\mathrm{d}T_{\mathrm{M}}(t)}{\mathrm{d}t} \quad U[T_{\mathrm{F}}(t) \quad T_{\mathrm{M}}(t)] \quad hA[T_{\mathrm{M}}(t) \quad T_{\infty}(t)] \tag{11}$$

where m_{M} is the moderator mass, C_{pM} – the moderator heat capacity, h – the convective heat transfer coefficient, and T_{∞} (t) – the coolant mean temperature.

Taking the reactor to be in a steady-state at $t = 0$ we get

$$C(0) \quad \frac{\beta}{\lambda \Lambda} n(0) \tag{12}$$

$$T_{\mathrm{m}}(0) \quad \frac{n(0) \quad hAT_{\infty}(0)}{hA} \tag{13}$$

$$T_{\mathrm{F}}(0) \quad \frac{n(0)}{U} \quad T_{\mathrm{m}}(0) \tag{14}$$

where A is the moderator-coolant contact surface.

Table 2 represents the initial conditions computed using the previous relations. The obtained values seem to be in agreement with the results reported by Li *et al*. [2]. In order to simplify the equations we define four new variables

$$x(t) \quad \frac{n(t) \quad n(0)}{n(0)} \tag{15}$$

Table 2. Initial conditions

$n(0)$ [W]	$T_{\mathrm{f}}(0)$ [°C]	$T_{\mathrm{m}}(0)$ [°C]
$1.00\ 10^2$	$8.53\ 10^2$	827.6

$$y(t) \quad \frac{C(t) \quad C(0)}{C(0)} \tag{16}$$

$$z_{\mathrm{M}}(t) \quad T_{\mathrm{M}}(t) \quad T_{\mathrm{M}}(0) \tag{17}$$

$$z_{\mathrm{F}}(t) \quad T_{\mathrm{F}}(t) \quad T_{\mathrm{F}}(0) \tag{18}$$

$$z_{\infty}(t) \quad T_{\infty}(t) \quad T_{\infty}(0) \tag{19}$$

Replacing the variables in eqs. (4, 5, 9, and 11) with the new variables we get

$$\frac{\mathrm{d}x(t)}{\mathrm{d}t} \quad \frac{\rho(t) \quad \beta}{\Lambda} x(t) \quad \frac{\beta}{\Lambda} y(t) \quad \frac{\rho(t)}{\Lambda} \tag{20}$$

$$\frac{\mathrm{d}y(t)}{\mathrm{d}t} \quad \lambda[x(t) \quad y(t)] \tag{21}$$

$$\frac{\mathrm{d}z_{\mathrm{F}}(t)}{\mathrm{d}t} \quad \frac{n(0)}{m_{\mathrm{F}} C_{p\mathrm{F}}} x(t) \quad \frac{kN_{\mathrm{fp}}}{m_{\mathrm{F}} C_{p\mathrm{F}}} [z_{\mathrm{F}}(t) \quad z_{\mathrm{M}}(t)] \tag{22}$$

$$\frac{\mathrm{d}z_{\mathrm{M}}(t)}{\mathrm{d}t} \quad \frac{kN_{\mathrm{fp}}}{m_{\mathrm{M}} C_{p\mathrm{M}}} [z_{\mathrm{F}}(t) \quad z_{\mathrm{M}}(t)] \quad \frac{hA}{m_{\mathrm{M}} C_{p\mathrm{M}}} [z_{\mathrm{M}}(t) \quad z_{\infty}(t)] \tag{23}$$

It is worth mentioning that in eqs. (22) and (23), the terms m_{M}, h, m_{F}, and k are functions of either the total number of pebbles or the number of fuel particles inside the reactor core, which in turn are related to the reactivity. In order to achieve a linear equation, the next part will focus on the temperature and reactivity dependence of each of the parameters present in the abovementioned equations.

COEFFICIENTS AND PARAMETERS ANALYSIS

Thermal properties of helium and their dependence on temperature should be evaluated. Per the KTA 3102 safety standard notation, the convective heat transfer rate and heat transfer coefficient – obtained using the pi theorem could be expressed as

$$Q \quad \alpha A(T_{\mathrm{F}} \quad T_{\infty}) \tag{24}$$

where

$$\alpha \quad \frac{\mathrm{Nu}\,\lambda_{\mathrm{g}}}{d} \tag{25}$$

where A is the surface area of the moderator region in contact with the coolant. The Nusslet number for packed bed reactors and the helium heat transfer coefficient are defined as [15]

$$\mathrm{Nu} \quad 1.27 \frac{\mathrm{Pr}^{1/3}}{\varepsilon^{1.18}} \mathrm{Re}^{0.38} \quad 0.033 \frac{\mathrm{Pr}^{1/2}}{\varepsilon^{1.07}} \mathrm{Re}^{0.86} \tag{26}$$

$$\lambda \quad 2.682\ 10^{-3}(1 \quad 1.123\ 10^{-3} P) T^{0.71(1 \quad 2\ 10^{-4} P)} \tag{27}$$

where

$$\mathrm{Re} \quad \frac{\frac{m}{A} d}{\eta} \tag{28}$$

$$\eta \quad 3.674\ 10^{-7} T^{0.7} \tag{29}$$

$$\mathrm{Pr} \quad \frac{C_p \eta}{\lambda_g} \tag{30}$$

The variations of the helium convective heat transfer coefficient are presented in fig. 8.

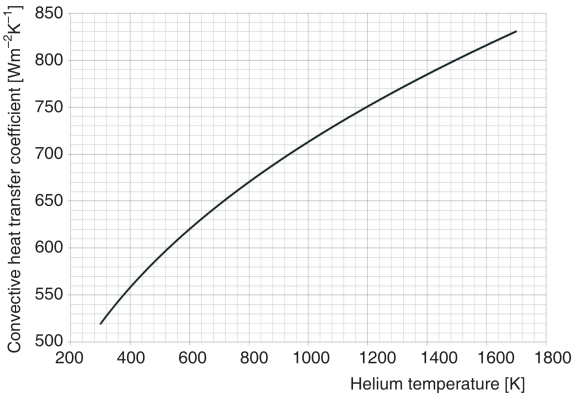

Figure 8. Temperature-dependent helium convective heat transfer coefficient

The heat capacities of both the fuel and graphite matrix were obtained according to the following formulas [16]

$$C_{p,\mathrm{UO_2}} \quad \frac{C_1 \theta^2 \mathrm{e}^{\theta/T}}{T^2 (e^{\theta/T} \quad 1)^2} \quad 2C_2 T \quad \frac{C_3 E_a \mathrm{e}^{\ E_a/T}}{T^2} \tag{31}$$

$$C_{p,grph} \quad 2.031 \quad 7.8645\ 10^{-5} T^2 \quad 4.2671\ 10^{-5} T^{-1} \quad 1.3203\ 10^{-8} T^{-3} \quad 1.199\ 10^{-10} T^{-4} \quad 298 \quad T \quad 1273\,\mathrm{K} \tag{32}$$

$$C_{p,grph} \quad 1.131 \quad 6.62\ 10^{-4} T \quad 9.969\ 10^{-8} T^2 \quad 1273 \quad T \quad 3273\,\mathrm{K} \tag{33}$$

where C_1, C_2, C_3, θ, and E_a are constants further represented in tab. 3 [17].

As obvious from figs. 9 and 10, both parameters are temperature-dependent. Their values at computed steady-state temperatures, as well as the effect of a 100 K deviation in temperature, are listed in tab. 4.

Table 3. Uranium oxide heat capacity correlation constants

Constant	Value	Units
C_1	296.7	[Jkg^{-1}K^{-1}]
C_2	2.43 10^{-2}	[Jkg^{-1}K^{-2}]
C_3	8.745 10^{7}	[Jkg^{-1}]
θ	535.285	[K]
E_a	1.577 10^{5}	[Jmol^{-1}]

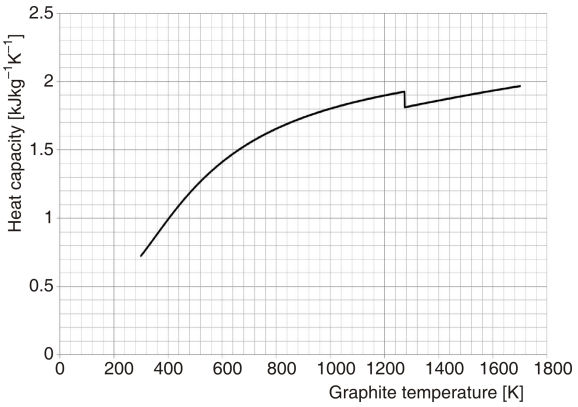

Figure 9. Temperature-dependent graphite heat capacity

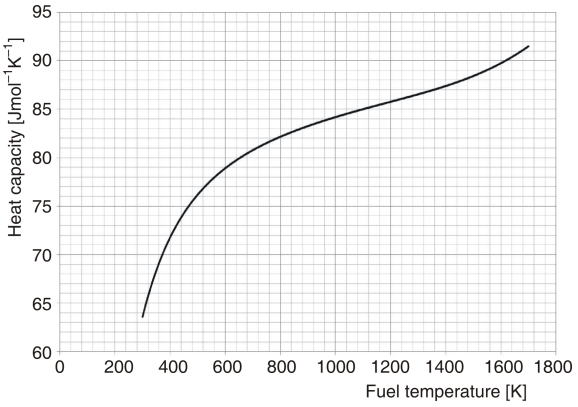

Figure 10. Temperature-dependent UO_2 heat capacity

Table 4. Graphite and uranium oxide heat capacities

Temperature	Graphite specific heat capacity	Uranium oxide specific heat capacity
1000 K	1803	–
1100 K	1855.9	–
1200 K	1899.7	–
1116 K	–	313.1
1126 K	–	316.1
1226 K	–	318.9

A variation of 100 K causes the heat capacities of the fuel and moderator to shift, respectively, by less than 1 % and 3 %. Hence, taking constant fuel and moderator heat capacities is an acceptable approximation.

As previously mentioned, four of the terms appearing in eqs. (21) and (22) are reactivity-dependent

$$A \quad 4\pi N_p R^2 \tag{34}$$

$$m_{\mathrm{F}} \quad \frac{4 \ 8335}{3} \rho_{\mathrm{F}} \pi \xi N_p r^3 \tag{35}$$

$$m_{\mathrm{M}} \quad \frac{4}{3} \pi N_p R^3 \tag{36}$$

and N_p itself, where N_p is the total number of pebbles inside the core, R [cm] – the pebble radius, ξ – the fuel to total pebble ratio, and ρ_F [gcm^{-3}] – the UO_2 density.

All of these terms eventually cancel each other out except ξ. Hence, one could take the ratio to be a constant and rewrite eqs. (22) and (23) as

$$\frac{dz_F(t)}{dt} \quad \frac{n(0)}{m_F C_{pF}} x(t) \quad \frac{k}{4\pi\rho_F C_{pF} r^3}[z_F(t) \quad z_M(t)] \tag{37}$$

$$\frac{dz_M(t)}{dt} \quad \frac{3\ 8335\ k\xi}{4\pi R^3 \rho_M C_{pM}}[z_F(t) \quad z_M(t)] \quad \frac{3h}{\rho_M C_{pM} R}[z_M(t) \quad z_\infty(t)] \tag{38}$$

Eqs. (37) and (38) are the final forms of the temperature feedback relations. The values of all the parameters discussed above are listed in tab. 5.

Table 5. Numerical values of the HTR-10 main parameters

Constant	Value	Constant	Value
C_{pF}	316.1063 J/kgK	R	0.00025 m
C_{pM}	1855.9 J/kgK	ξ	0.57
ρ_F	10400 kg/m^3	Λ	0.00168 s
ρ_M	1730 kg/m^3	β	0.00726
h	657.7343 J/Km^2	λ	0.08 s^{-1}
$\dot{m}$	4.32 kg/s	P	3.0 MPa
T_∞	748 K	R	0.03 m

In this form, we have two forcing functions – or potential system inputs – which are the excess reactivity $\rho_0(t)$ and the coolant mean temperature $z_\infty(t)$. The mean coolant temperature used in this formulation does not correspond to any controllable physical parameter in the reactor.

RESULTS AND DISCUSSION

Radioactive material leakage into the coolant cycle is one of the most pressing issues in the safety and design of solid fuel reactors. Apart from the solid fuel itself, the cladding (here, for PBM-type reactors, the TRISO coating) is the only barrier preventing leakage into the coolant. The failure rate is highly dependent on the reactor temperature. High working temperatures and sudden temperature bursts can all contribute to a higher cladding failure rate. As reactivity changes are very common in reactor operation and usually accompanied with an increase in both fuel and moderator temperatures, a thorough investigation of the reactor's dynamic behavior upon reactivity insertion and coolant temperature variation could help fix the safe operation margins and demonstrate the reactor's inherent safety. In order to benchmark the model, at t = 50 s, a 0.05 \$ (1 \$ = β $\Delta k/k$) reactivity change was introduced. The system response to the aforementioned step-function is displayed in figs. 11 and 12.

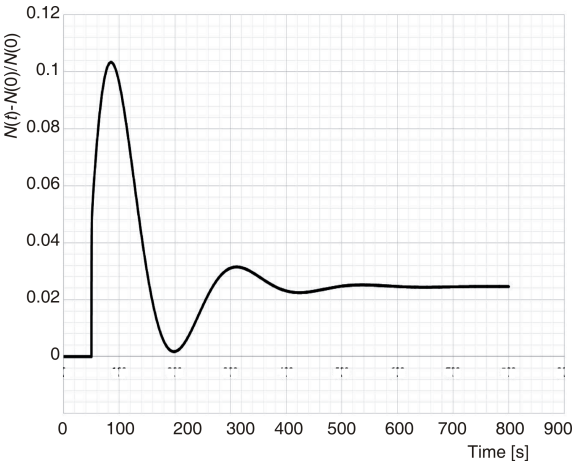

Figure 11. Reactor power variation induced by 0.05 \$ reactivity insertion

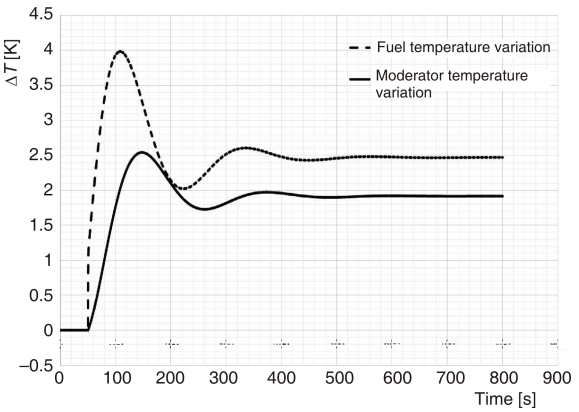

Figure 12. Fuel and moderator temperature variation induced by 0.05 \$ reactivity insertion

The obtained results seem to agree with the simulation performed by Li *et al*. Some of the main characteristics of the system response are listed and compared in tab. 6.

Table 5 points out a 10 s to 20 s second lag in our system's response time along with a 10 % underestimation of the reactor power and core temperature as

Table 6. System response to 0.05 \$ step reactivity input

Parameter	The present study		Li *et al.*
Power peak	10.5 %		12.9 %
First response time	35 s		25 s
Reactor core temperature variation peak	Fuel	Moderator	5 °C
	4 °C	2.6 °C	
First response time	60 s	100 s	75 s

compared to the reference. This is due to the many simplifications made in the present model (such as the reduced number of nodes, constant temperature coolant assumption, *etc*.) and the difference in initial steady-state reactor power – 10 MW in this study, while 10.1 MW for the reference.

Figures 13, 14, and 15 represent the reactor's response to 0.25 $, 0.5 $, and 1 $ reactivity insertion. According to figs. 14 and 15, at 1 $ the fuel temperature exhibits an initial spike of 100 K before converging to its final value. As illustrated in fig. 16, the amplitude of this initial spike increases steadily with increasing reactivity – going from around 4 K to 100 K. At 1 $ it takes the fuel heat dissipation mechanism approximately 10 seconds to counter the effect of the excess in reactivity. This fairly short response time is due to the high number of fuel particles and, hence, high surface area in the pebbles. Once the conduction mechanism has kicked in, the heat starts to pile up in the moderator causing it to reach a maximum of 50 K which, due to the high amount and heat capacity of graphite, is far less than the fuel maximum temperature 60 seconds later.

The current work has tried to establish a simple dynamic model for pebble-bed type reactors based on

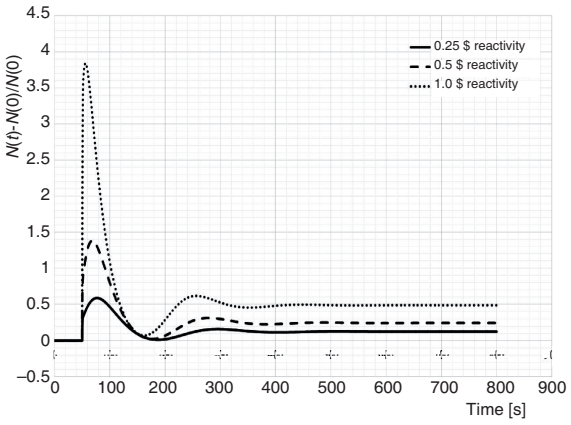

Figure 13. Reactor power response to 0.25 $, 0.5 $, and 1 $ reactivity insertion

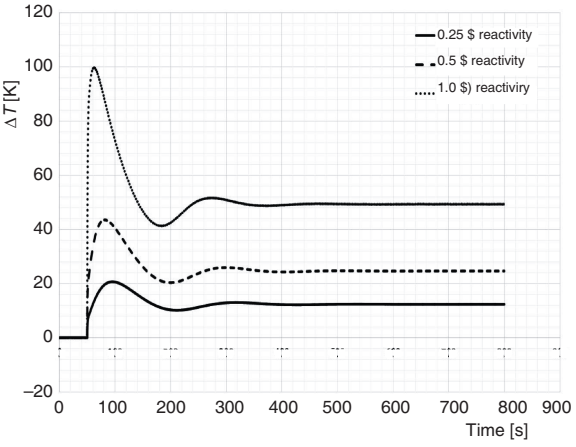

Figure 14. Fuel temperature response to 0.25 $, 0.5 $, and 1 $ reactivity insertion

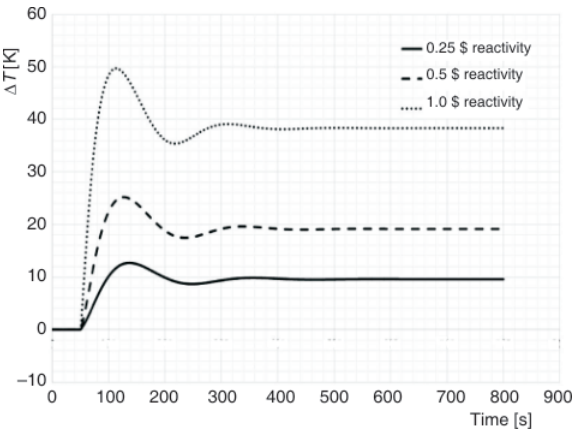

Figure 15. Moderator temperature response to 0.25 $, 0.5 $ and 1 $ reactivity insertion

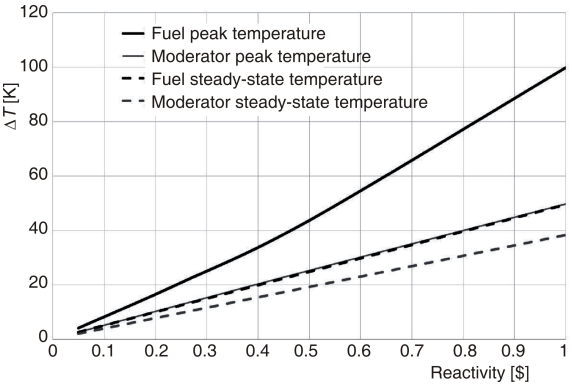

Figure 16. Reactor core temperature as a function of reactivity

the single-region point kinetic equation and two-way temperature feedbacks. The results obtained in fig. 16 are in partial agreement with some of the results in a previously proposed model. The model shows a small lag as compared to the reference model while underestimating (by less than 10 %) the amplitude of the initial spikes. These differences are mainly due to the differences in the models, for example, this model does not take account of changes in coolant pressure and temperature. The results obtained through the modeling, while in partial agreement with previously proposed models, have highlighted the system's inherent safety.

REFERENCES

[1] Hosseini, S. A., Basiri, H., Athari Allaf, M., Evaluation of the Chinese Pebble Bed Reactor's Temperature Reactivity Coefficients, in: Computational Physics Conference of Iran, Tehran, 2013, pp. 131-134

[2] Li, H., Huang, X., Zhang, L., A Simplified Mathematical Dynamic Model of the HTR-10 High Temperature Gas-Cooled Reactor with Control System Design Purposes, *Ann. Nucl. Energy, 35* (2008), 9, pp. 1642-1651

[3] Faghihi, F., Fadaie, A. H., Sayareh, R., Reactivity Coefficients Simulation of the Iranian VVER-1000 Nu-

clear Reactor Using WIMS and CITATION Codes, *Prog. Nucl. Energy, 49* (2007), 1, pp. 68-78
[4] Haneklaus, N., Transuranic Waste Incineration Using High Temperature Pebble Bed Reactors, University of Ljubljana, Ljubljana, 2013
[5] Hosseini, S. A., Athari Allaf, M., Pebble Bed Reactors Simulation Using MCNP: The Chinese HTR-10 Reactor, *Iran. J. Phys. Res., 13* (2013), 2, pp. 177-182
[6] Lopez Aldama, D., Nichols, A. L., ADS-2.0: A Test Library for Accelerator Driven Systems and New Reactor Designs, INDC (NDS)-0545 [R/OL], IAEA, Vienna, Austria, 2008
[7] Chadwick, M. B., *et al*., ENDF/B-VII. 0: Next Generation Evaluated Nuclear Data Library for Nuclear Science and Technology, *Nucl. Data Sheets, 107* (2006), 12, pp. 2931-3060
[8] Hosseini, S. A., Athari Allaf, M., Implementation and Benchmarking of ENDFVII Based Library for PBM Reactor Analysis with MCNP4c, *Prog. Nucl. Energy, 60* (2012), pp. 27-30
[9] Hu, S., Wang, R., Gao, Z., Safety Demonstration Tests on HTR-10, in 2nd International Topical Meeting on High Temperature Reactor Technology, Beijing, China, 2004, pp. 22-24
[10] Hosseini, S. A., Athari Allaf, M., Benchmarking of the HTR-10 Reactor's Kinetic Parameters: Effective Delayed Neutron Fraction, *Prog. Nucl. Energy, 75* (2014), pp. 80-91
[11] Hosseini, S. A., A New Random Distribution Method to Simulate PBM Type Reactors with MCNP, *Ann. Nucl. Energy, 50* (2012), pp. 215-219
[12] Methnani, M., Coordinated Research Programme on Evaluation of High Temperature Gas Cooled Reactor Performance: Benchmark Analysis Related to the PBMR-400, PBMM, GT-MHR, HTR-10 and the ASTRA Critical Facility, IAEA, Vienna, Austria, 2006
[13] Lamarsh, J. R., Introduction to Nuclear Reactor Theory, Addison-Wesley, Boston, Mass, USA, 1966
[14] Lamarsh, J. R., Baratta, A. J., Introduction to Nuclear Engineering, vol. 3. Prentice Hall, N. J., USA, 2001
[15] ***, KTA, Reactor Core Design of High Temperature Gas-cooled Reactors: Heat Transfer Spherical Fuel Elements, Nucl. Saf. Stand. Com. Ger., 1983
[16] Bobkov, V. P., *et al*., Thermophysical Properties of Materials for Nuclear Engineering: A Tutorial and Collection of Data, IAEA, Vienna, 2008
[17] Luscher, W. G., *et al*., Material Property Correlations: Comparisons between FRAPCON-3.4, FRAPTRAN 1.4, and MATPRO. US Nuclear Regulatory Commission, Office of Nuclear Regulatory Research, 2011

Received on May 24, 2015
Accepted on June 2, 2015

Сеј̄ед Али ХОСЕИНИ

ДИНАМИЧКО ПОНАШАЊЕ HTR-10 РЕАКТОРА – МОДЕЛ ДВОЈНЕ ТЕМПЕРАТУРНЕ ПОВРАТНЕ СПРЕГЕ

Намера је да се у раду прикаже једноставан модел анализе динамичког понашања реактора са сферним горивним елементима. Предложени модел заснива се на једначинама тачкасте кинетике са температурном повратном спрегом на температуре горива и модератора. Коефицијенти температурне реактивности добијени су MCNP кодом и из расположивих експерименталних података. Параметри топлотне капацитивности и топлотне проводљивости пажљиво су анализирани и коначни систем једначина решен је нумерички. Добијени резултати, поред делимичне сагласности са раније предложеним моделима, у поређењу са другим пројектима реактора, упућују на нижу осетљивост при скоковитом уносу реактивности и на инхерентну сигурност.

Кључне речи: HTR-10, модел тачкасте кинетике, коефицијент температурне реактивности, MCNP, модуларни реактор са сферним горивним елементима